A new dual earthquake and submarine landslide source model for the 28 September 2018 Palu (Sulawesi), Indonesia tsunami

Mohammad Heidarzadeh[*1], Iyan E. Mulia[2,3]

[1] Department of Architecture and Civil Engineering, University of Bath, Bath BA2 7AY, UK.

[2] Prediction Science Laboratory, RIKEN Cluster for Pioneering Research, 7-1-26 Minatojima-minami-machi, Chuo-ku, Kobe, Hyogo 650-0047, Japan.

[3] Disaster Resilience Science Team, RIKEN Center for Advanced Intelligence Project, 1-4-1 Nihonbashi, Chuo-ku, Tokyo 103-0027, Japan.

Published in: "**Coastal Engineering Journal**"

https://doi.org/10.1080/21664250.2022.2122293

*** Correspondence to:**
Mohammad Heidarzadeh, PhD
Associate Professor
Department of Architecture and Civil Engineering,
University of Bath, Bath BA2 7AY,
United Kingdom.
Email: mhk58@bath.ac.uk
Website: https://researchportal.bath.ac.uk/en/persons/mohammad-heidarzadeh-kolaei
ORCID: https://orcid.org/0000-0002-1112-1276

Abstract (200 words)

The September 2018 Palu (Sulawesi, Indonesia) tsunami has been a heavily debated event because multiple source models of three different types have been proposed for this tsunami: (i) The M_w 7.5 earthquake, (ii) Landslides, and (iii) Dual earthquake and landslide. Surprisingly, all of these three types of models were reported successful in the literature in terms of reproducing the existing tsunami observations. This can be partly attributed to the limited observations available for this tsunami. This study is motivated by the results of a marine bathymetric survey, which identified evidence for submarine landslides within the Palu Bay. Our modelling shows that the tsunami cannot be exclusively attributed to the M_w 7.5 earthquake. Inspired by the results of the marine survey, we propose a dual source model including a submarine landslide although most of the existing models include subaerial coastal landslides. Our dual model comprises of an earthquake model, which has a length of 264 km, a width of 37 km and a slip of 0 – 8.5 m, combined with a submarine landslide with a length of 1.0 km, a width of 2.0 km and a thickness of 80.0 m located at 119.823 ^{o}E and -0.792 ^{o}S.

Keywords: Tsunami; Earthquake; Submarine Landslide; Palu; Numerical Modelling.

1. Introduction

The Palu city in Sulawesi of Eastern Indonesia was struck by a destructive tsunami following an M_w 7.5 strike-slip earthquake on 28 September 2018 (Figure 1), which together killed more than 4,000 people. The earthquake origin time was reported as 10:02:45 (UTC) with a depth of 20.0 km and an epicentre at -0.256°S and 119.846°E by the United States Geological Survey (USGS, 2018). The Palu earthquake and tsunami produced the largest natural disaster in Indonesia following the 2004 Indian ocean tsunami. Some other natural disaster in Indonesia in the aftermath of the 2004 event are the July 2006 Pangandaran earthquake (M_w 7.7) and tsunami with over 800 deaths (Fujii and Satake, 2006), the October 2010 Mentawai earthquake (M_w 7.7) and tsunami with 408 fatalities (Satake et al., 2013, 2020), and the December 2018 Anak Krakatau volcano tsunami with over 450 casualties (Grilli et al., 2021; Heidarzadeh et al., 2020; Mulia et al., 2020).

Possibly the 2018 Palu tsunami could be considered as one of the most debated tsunamis in terms of its source mechanism in the past few decades because different types of source models and in a large number have been proposed for this event, which sometimes contradict each other. Some of these models are given in Table 1. While some authors attributed the tsunami to only its earthquake source (an M_w 7.5 strike-slip event), others completely ignored the earthquake source of the event and proposed that the tsunami was due to landslides (Table 1). Approximately four years after the 2018 Palu event and thanks to several field works and numerous modelling efforts, it is possibly fair to claim that there is a consensus in the tsunami community that the 2018 Palu tsunami was the result of

63 a dual source, i.e., combined earthquake and landslide. There are several evidence for both co-seismic
64 crustal deformation (e.g., field surveys by Natawidjaja et al., 2021) and submarine/subaerial landslides
65 (e.g., marine surveys by Frederik et al., 2019; coastal surveys of Takagi et al., 2019, Aránguiz et al.
66 2020 and Liu et al., 2020). Despite multiple efforts (Table 1) to characterise the earthquake and
67 landslide sources of the tsunami separately, the topic is still open, and more research efforts are
68 required as recommended by some authors listed in Table 1. Therefore, the purpose of this research is
69 to offer a realistic dual source model that is able to satisfactorily reproduce the existing tsunami
70 observations (i.e., tide gauges and runup surveys) and address some of the shortcomings (discussed in
71 the next Section) of the existing source models. We use data from the bathymetric survey of Frederik
72 et al. (2019) to identify a potential submarine landslide source responsible for the Palu event combined
73 with published seismic source models to propose our dual model. We apply numerical modelling to
74 validate our source model through comparing tsunami modelling results with observed tide gauge data
75 and surveyed runup heights.
76

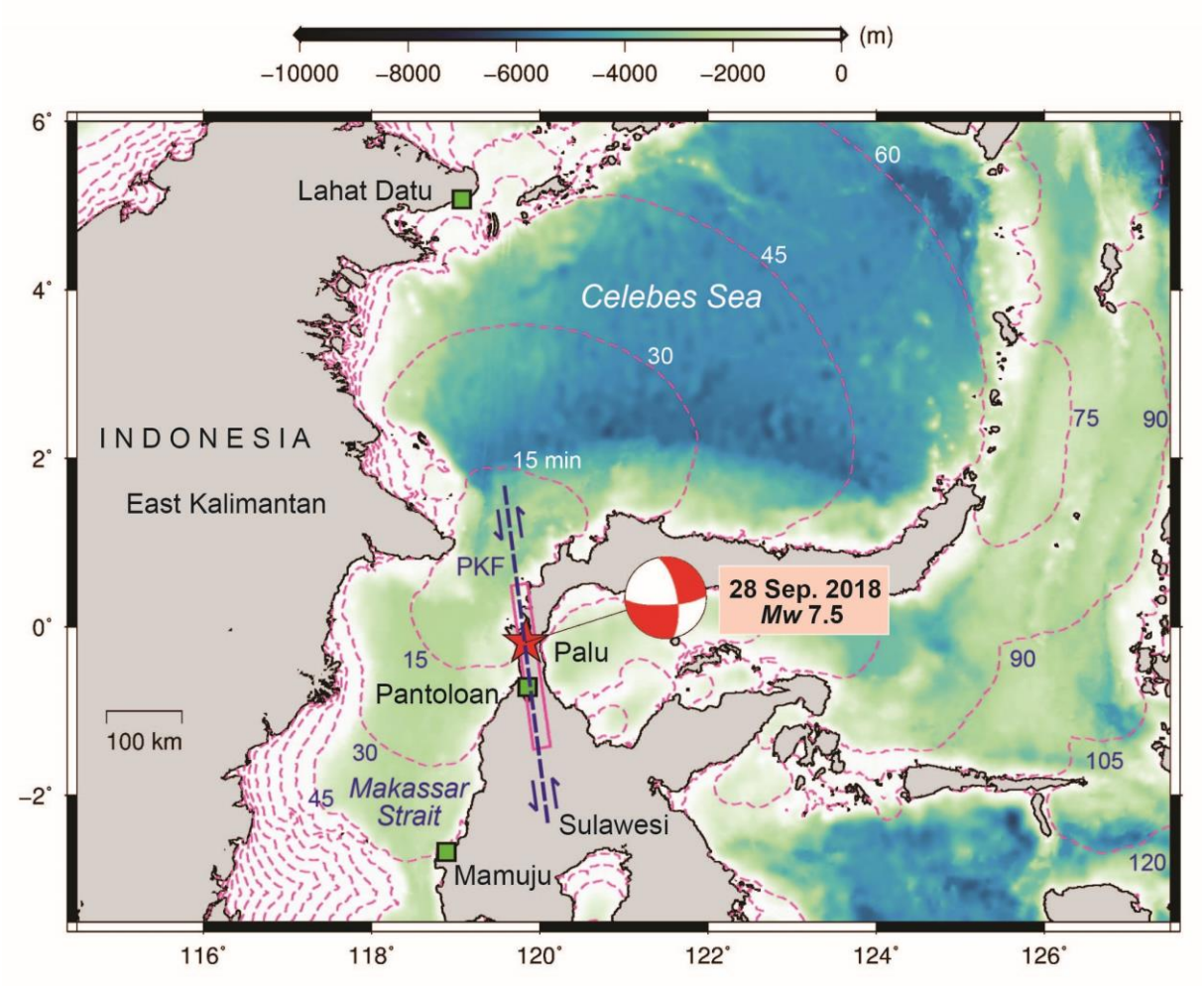

Figure 1. Map showing Eastern Indonesia, the site of the 28 September 2018 Palu (Sulawesi) earthquake and tsunami. The red star indicates the epicenter of the earthquake, the green squares are the locations of tide gauge stations, and the dashed contours show the tsunami travel times (TTT) in minutes calculated using the TTT software of Geoware (2011). The Palu-Koro strike-slip fault system (PKF) is shown by a dashed thick straight line. The focal mechanism is based on the United States Geological Survey (USGS) catalogue. The pink rectangle demonstrates the fault extension for the 2018 Palu earthquake based on Lee et al. (2019).

2. A brief review of existing source models and our objectives

There have been extensive controversies in the past few years over the source mechanism of the 2018 Palu earthquake and tsunami and multiple hypotheses have been proposed. Three different types

89 of source models were proposed for this event (Table 1) comprising, (i) Only-earthquake models (i.e.,
90 the coseismic crustal deformation), (ii) Only-landslide models (i.e., submarine or subaerial mass
91 failures triggered by the earthquake), and (iii) Dual models (i.e., combined earthquake and landslide).
92 Heidarzadeh et al. (2019) were among the first authors who showed that the tsunami was most likely
93 the product of a combined earthquake and submarine landslide sources, and they approximated the
94 location of a potential submarine landslide. Tsunami inversion by Gusman et al. (2019) revealed that
95 an additional submarine landslide source is necessary to explain the observed inundation limits.
96 Among the only-landslide models are those proposed by Pakoksung et al. (2019) and Nakata et al.
97 (2020), who considered several hypothetical landslides and applied numerical modelling to show that
98 some of them could be possible. On the other hand, Ulrich et al. (2019) and Jamelot et al. (2019)
99 proposed models involving only earthquake ruptures. Among authors who proposed dual sources are
100 Heidarzadeh et al. (2019), Williamson et al. (2020) and Schambach et al. (2021) (Table 1).

101 Several field surveys were conducted following the event to record coastal tsunami heights and
102 damage (Muhari et al., 2018; Arikawa et al., 2018; Omira et al., 2019; Syamsidik et al., 2019). A
103 marine bathymetric survey was conducted by Frederik et al. (2019) following the event to map
104 potential bathymetric changes in the Palu Bay. Takagi et al. (2019) and Liu et al. (2020) mapped
105 several coastal landslides in the area through field surveys. All these field data of different types
106 confirmed that the tsunami source was most likely generated by a dual source, comprising the M_w 7.5
107 strike-slip earthquake and landslides (submarine or subaerial). However, the current knowledge on a

potential dual model for the 2018 Palu event is limited. There are three studies that proposed dual models: Heidarzadeh et al. (2019), Williamson et al. (2020) and Schambach et al. (2021). The study by Heidarzadeh et al. (2019) gives only the location of a potential submarine landslide without offering its dimensions or details. The two latter models are based on onshore subaerial landslides in their dual models with the exception that Williamson et al. (2020) also considered a hypothetical submarine landslide at the location previously proposed by Heidarzadeh et al. (2019) (Table 1). While there is evidence that such onshore subaerial landslides occurred (e.g., Takagi et al., 2019; Aránguiz et al. 2020; Liu et al., 2020), there are also evidence that submarine landslides were involved (e.g., marine bathymetric survey of Frederik et al., 2019; Heidarzadeh et al., 2019). Therefore, the shortcomings of the existing dual models are: (i) Credible submarine landslides are missing in existing dual models although Heidarzadeh et al. (2019) proposed a hypothetical submarine landslide; and (ii) The simulated waves from landslide sources within the existing dual models show a mix of short and long waves as compared to the observed waveform in Pantoloan, and does not match the observations well.

Due to the relatively small sizes of coastal subaerial landslides, which result in some shorter-period waves compared to observations in Pantoloan, it is likely that a large submarine landslide was involved that could produce longer-period waves in Pantoloan. Marine surveys of Frederik et al. (2019) give evidence for such a large submarine landslide. The purpose of this research is to consider such a credible submarine landslide in our dual model. While we acknowledge that the dual source models proposed by Heidarzadeh et al. (2019), Williamson et al. (2020) and Schambach et al. (2021)

127 are important contributions, this study seeks to further complement them by considering a potential
128 reliable submarine landslide.

129 It is important to note that due to the limited tsunami observation data for the 2018 Palu event,
130 many models of different types (earthquake, landslide and dual models) can reproduce the
131 observations. Therefore, the purpose of this study is not to discredit any of the published models.
132 Rather, we aim at offering an alternate dual model that is supported by existing observation data.

133

134 **Table 1.** A list of some of the published source models for the September 2018 Palu (Sulawesi)
135 tsunami.

136

Type of source model	Author	Type of tsunami data for validation	Description
Earthquake	Ulrich et al. (2019)	Tide gauge and runup survey	A slip model is proposed based on teleseismic inversion
	Jamelot et al. (2019)	Tide gauge and runup survey	A slip model is proposed based on optical image correlation, and the geological and tectonic context
	Bacques et al. (2020)	None	A slip model is proposed based on space-based geodetics measurements of the co-seismic displacement field
	Yolsal-Çevikbilen and Taymaz (2019)	None	A source model is proposed based on inversion of teleseismic body waves
	He et al. (2019)	None	A slip model is proposed based on far-field InSAR, near-field SAR and optical sub-pixel correlation data
	Lee et al. (2019)	None	A slip model is proposed based on teleseismic inversion
Landslide	Pakoksung et al. (2019)	Tide gauge and runup survey	Ten landslide sources of various sizes (small and large) ae proposed, which are spread all along the Palu Bay.
	Nakata et al. (2020)	Tide gauge and runup survey	Several models are tested. The preferred model is comprised of two landslides within the Palu Bay
	Liu et al. (2020)	Tide gauge	Several coastal landslides are considered as the tsunami source
	Nagai et al. (2021)	Tide gauge and runup survey	Several coastal landslides are considered as the tsunami source
	Somphong et al. (2022)	Tide gauge and runup survey	Several submarine and coastal landslides are considered as the tsunami source
	Aránguiz et al. (2020)	Tide gauge	A few landslides are considered as the source
	Takagi et al. (2019)	Eyewitnesses	A landslide was considered as the source
Dual (earthquake and	Heidarzadeh et al. (2019)	Tide gauge	The tsunami is modelled based on a coseismic slip model and it was shown that an additional submarine landslide source is necessary. The location for the submarine

landslide)			landslide is determined as south of the Palu Bay.
	Schambach et al. (2021)	Tide gauge and runup survey	A combination of a coseismic slip model and several coastal landslides is considered as the dual model.
	Williamson et al. (2020)	Tide gauge and runup survey	A combination of a coseismic slip model, several coastal landslides, and a hypothetical submarine landslide (at the location previously proposed by Heidarzadeh et al. 2019) is considered as the dual model
	This study	Tide gauge and runup survey	A combination of a coseismic slip model and a single submarine landslide is considered as the dual model

3. Data and methods

The data used in this study comprises tide gauge records and runup heights of the tsunami, seismic source models for the 2018 Palu earthquake published by other studies, and the bathymetric survey data of the Palu Bay in the aftermath of the tsunami acquired by the marine survey of Frederik et al. (2019).

Tide gauge data of the tsunami at three stations (Pantoloan, Mamuju and Lahat Datu) (Figure 1), are used in this study. The records of Pantoloan and Mamuju are provided by the Indonesia Agency for Geo-spatial Information (http://big.go.id) whereas that of Lahat Datu is from the sea level monitoring facility of the Intergovernmental Oceanographic Commission (http://www.iocsealevelmonitoring.org/). All sea level data are sampled at 1 min intervals. These sea level records were previously analysed and de-tided by Heidarzadeh et al. (2019) (Figure 2b).

For the seismic source models of the event, we use three models published by USGS (2018), Jamelot et al. (2019) and Wang et al. (2019) (Table 2). We acknowledge that multiple seismic source models were published for the 2018 Palu earthquake by different authors in the past few years (Table

152 1). Here, we use three of such source models in order to test a range of models and compare their
153 performances in reproducing the observations. Table 2 gives the fault parameters for these three
154 models, indicating that the maximum slip values for them are 8.5 m (USGS, 2018), 8.0 m (Jamelot
155 et al., 2019), and 3.9 m (Wang et al., 2019). Here, the dislocation model of Okada (1985) is used to
156 calculate coseismic crustal deformation using the fault parameters listed in Table 2 for the three
157 earthquake source models (Figure 2a). The calculated crustal deformations (Figure 2a) are used as
158 initial conditions for tsunami modelling.

159 For defining the submarine landslide source models in this study, we use data from the actual post-
160 event marine bathymetric surveys conducted by Frederik et al. (2019), who identified some potential
161 landslides within the Palu Bay although the survey was unable to find clear evidence of recent land-
162 sliding associated with the 2018 Palu event. Consistent with the previous results by Heidarzadeh et al.
163 (2019), who reported two potential submarine landslide locations in the north (latitude of -0.67 ^{o}S) and
164 middle (latitude of -0.82 ^{o}S) of the Palu Bay, Frederik et al. (2019) also reported two potential
165 submarine landslide locations in the north and middle of the bay. By considering the results of several
166 post-event tsunami runup and height surveys (e.g., Muhari et al., 2018; Arikawa et al., 2018; Omira et
167 al., 2019; Syamsidik et al., 2019), it is very likely that the potential submarine landslide source was
168 located around the middle of the bay because it is the location of the largest surveyed runup heights
169 (Heidarzadeh et al., 2019). Therefore, from the study of Frederik et al. (2019), here we only consider
170 the potential landslide from the middle of the bay. In addition, we ignore the onshore subaerial

landslides in our study by assuming that the effects of such onshore landslides are negligible as compared to those of a large submarine landslide. However, we acknowledge that multiple onshore subaerial landslides occurred during the 2018 Palu event (e.g., Takagi et al., 2019).

Two transects of a potential landslide located around the middle of the Palu Bay (approximately 119.823 °E and -0.792 °S) are reported by Frederik et al. (2019) with a slope angle of 11 – 13° and thickness of 55 – 70 m. The two transects are distanced approximately 1,000 m. The length and width of the landslide cannot be precisely extracted from the report of Frederik et al. (2019) because the field data are limited; however, they can help us to approximate the length and width of the submarine landslide. Considering bathymetric data of Frederik et al. (2019), we assume the length of the landslide in the range of 500 – 1,000 m and consider two scenarios LS-1 (length of 1,000 m) and LS-2 (length of 500 m) in order to consider the uncertainty of length estimation in our study and to conduct a sensitivity analysis (Table 3). In fact, a length in the range of 500 – 1,000 m appears meaningful given the results of bathymetric surveys of Frederik et al. (2019); however, the final length is determined by comparing simulated waveforms with observations. The width of the landslide is considered as 2,000 m for both LS-1 and LS-2 scenarios guided by the field data of Frederik et al. (2019). Inspired by the marine survey of Frederik et al. (2019), landslide thicknesses of 80 m and 40 m are considered for LS-1 and LS-2, respectively (Table 3).

To generate the initial sea surface displacement due to submarine landslides, we apply the empirical equations of Watts et al. (2005), which are based on studies previously conducted by

190 Synolakis et al. (2002), Satake and Tanioka (2003), and Okal and Synolakis (2004). Figure 3a shows
191 the initial sea surface displacement due to the two landslide scenarios, which are employed as initial
192 conditions for tsunami simulations. Landslide tsunami modelling based on the empirical equations of
193 Synolakis et al. (2002) and Watts et al. (2005) is a static modelling approach, which implies that the
194 dynamic landslide generation process is overlooked. It has been shown by several authors that such an
195 approach is successful in reproducing past landslide tsunami events (e.g., Synolakis et al., 2002;
196 Tappin et al., 2008; Heidarzadeh and Satake, 2015, 2017).

197 Tsunami modelling in this study is performed applying the numerical package COMCOT (Cornell
198 Multi-grid Coupled Tsunami model) (Wang and Liu, 2006), which solves linear and nonlinear Shallow
199 water Equations on Cartesian and Spherical bathymetric and topographic grids. Nonlinear equations
200 were used in this study. We used the bathymetric and topographic grid provided by GEBCO (The
201 General Bathymetric Chart of the Oceans), which has an original spatial resolution of 15 arc-sec
202 (Weatherall et al., 2015). A single uniformly-spaced bathymetric grid with grid spacing of 10 arc-sec is
203 used in this study, which is re-sampled from the original GEBCO grid in order to provide a smaller
204 grid spacing for guaranteeing the stability of numerical computations. A grid size of 10 arcsec is
205 equivalent to approximately 300 m (around earth latitude of zero). By knowing that the sea surface
206 displacement field, according to the equations by Watts et al. (2005), is approximately three times of
207 the landslide dimensions, the grid size of 10 arcsec (300 m) implies that there are at least nine or 10
208 grid points for each landslide source (Figure 3a). Therefore, the resolution of the computational grid is

sufficient to carry out the computations. A time step of 0.5 s was employed to guarantee the stability of the numerical scheme based on the Courant-Friedrichs-Lewy criterion (Courant et al., 1928). The total simulation time was 4.5 h. To avoid uncertainties associated with wave amplitudes during nonlinear wave inundation on dry land, in this study we used tsunami amplitudes at the 1-m water depth contour as approximations of tsunami runup heights (e.g., Tinti et al., 2006; Pranantyo et al., 2021).

Three types of simulations were conducted: (i) Simulations based on the earthquake source of the tsunami for three candidate earthquake models EQ-1, EQ-2 and EQ-3 as listed in Table 2 and shown in Figure 2a; (ii) Simulation using two landslide sources LS-1 and LS-2 (Table 3, Figure 3a); (iii) Simulations for dual (combined earthquake and landslide) sources, Dual-1 and Dual-2, where the earthquake and landslide sources are superimposed simultaneously (Table 4; Figure 4a). The basis for defining our dual models is explained in the next section. For modelling dual sources, it is assumed that the earthquake and the submarine landslide occur simultaneously.

To measure the qualities of fit between observations (O_i) and simulations (S_i), we use the misfit equation developed by Heidarzadeh et al. (2022):

$$\epsilon = \frac{1}{N} \sum_{i=1}^{N} (O_i - S_i)^2 \quad (1)$$

where, $i = 1,2,3,\ldots,N$ is a counter for the points on a time series, O_i is an observation reading, S_i is the corresponding simulation reading, and N is the total number of points in the time series. When simulations coincide with observations (a perfect match), ϵ becomes zero, otherwise it increases by an

increase in mismatch between observations and simulations. We applied only the first tsunami wave in each station for misfit calculations.

Table 2. Earthquake source models used in this study for modelling the 28 September 2018 Palu (Sulawesi) earthquake and tsunami.

Model name	Author	Length (km)	Width (km)	Strike (°)	Dip (°)	Rake (°)	Depth (km)	Slip (m)
EQ-1	USGS (2018)	264	37	358.0	66.0	320.0 – 390.0	0.8 – 32.8	0 – 8.5
EQ-2	Jamelot et al. (2019)	138	12	2 – 357	45 – 69	11.0 – 38.0	5.6 – 6.3*	4.5 – 8
EQ-3	Wang et al. (2019)	210	20	316 – 359	67	(-99.1) – 179.3	0 – 25.2	0 – 3.9

*: For the source model proposed by Jamelot et al. (2019), the depths of the centre of the fault segments are reported.

Table 3. Parameters of the two landslide scenarios considered in this study for modelling the 28 September 2018 Palu (Sulawesi) tsunami.

Name	Long.[1] (°E)	Lat.[2] (°S)	Water depth (m)	Slope (°)	Length (m)	Width (m)	Thick.[3] (m)	Max. initial depr.[4] (m)	Max. initial elev.[5] (m)
LS-1	119.823	-0.792	500	12	1000	2000	80	9.7	7.8
LS-2	119.823	-0.792	500	12	500	2000	40	5.4	4.1

[1]: Longitude; [2]: Latitude; [3]: Thickness of the landslide; [4]: Maximum initial sea surface depression; [5]: Maximum initial sea surface elevation.

Table 4. Information of two dual earthquake and landslide source models considered in this study for modelling the 28 September 2018 Palu (Sulawesi) tsunami.

Name of the dual model	Components of the dual model	
	Earthquake model	Landslide model
Dual-1	EQ-1	LS-1
Dual-2	EQ-1	LS-2

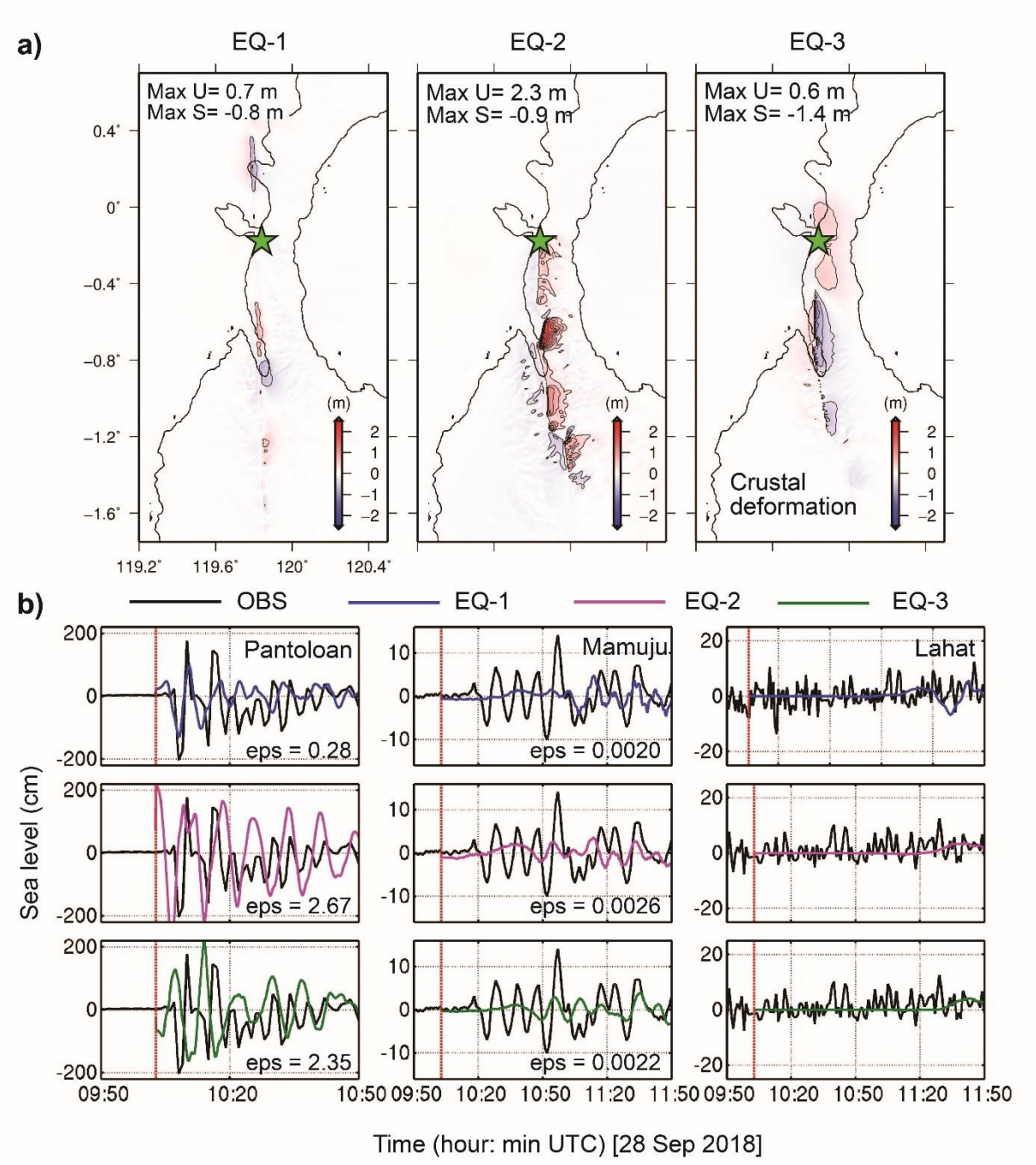

Figure 2. a) Three published seismic source models for the 28 September 2018 Palu (Sulawesi) M_w 7.5 earthquake namely EQ-1 (USGS, 2018), EQ-2 (Jamelot et al., 2019), and EQ-3 (Wang et al., 2019). **b)** Comparison of observed and modelled tsunami waveforms at three tide gauge stations due to the three aforementioned earthquake source models. "U" and "S" denote "uplift" and "subsidence", respectively. "eps" indicates misfit ϵ based on Equation (1). Misfits ("eps") are not calculated for Lahat as the tsunami signal is not clear at this station.

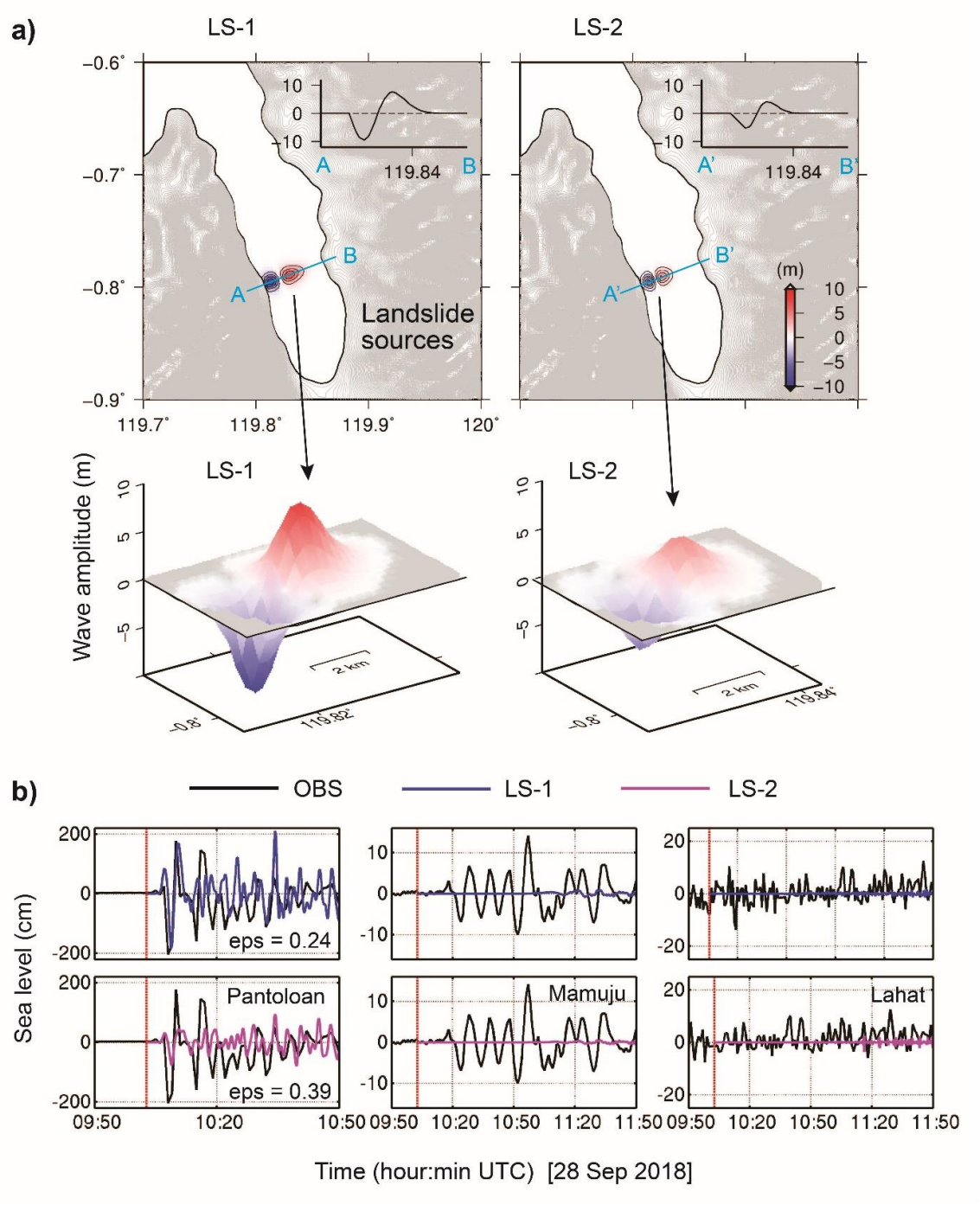

Figure 3. a) Two landslide models LS-1 and LS-2 considered in this study with corresponding initial sea surface displacements. **b)** Comparison of observed and modelled tsunami waveforms at three tide gauge stations due to the two aforementioned landslide scenarios. "eps" indicates misfit ϵ based on Equation (1). Misfits ("eps") are not calculated for Mamuju and Lahat as the simulated waves are very small at these stations.

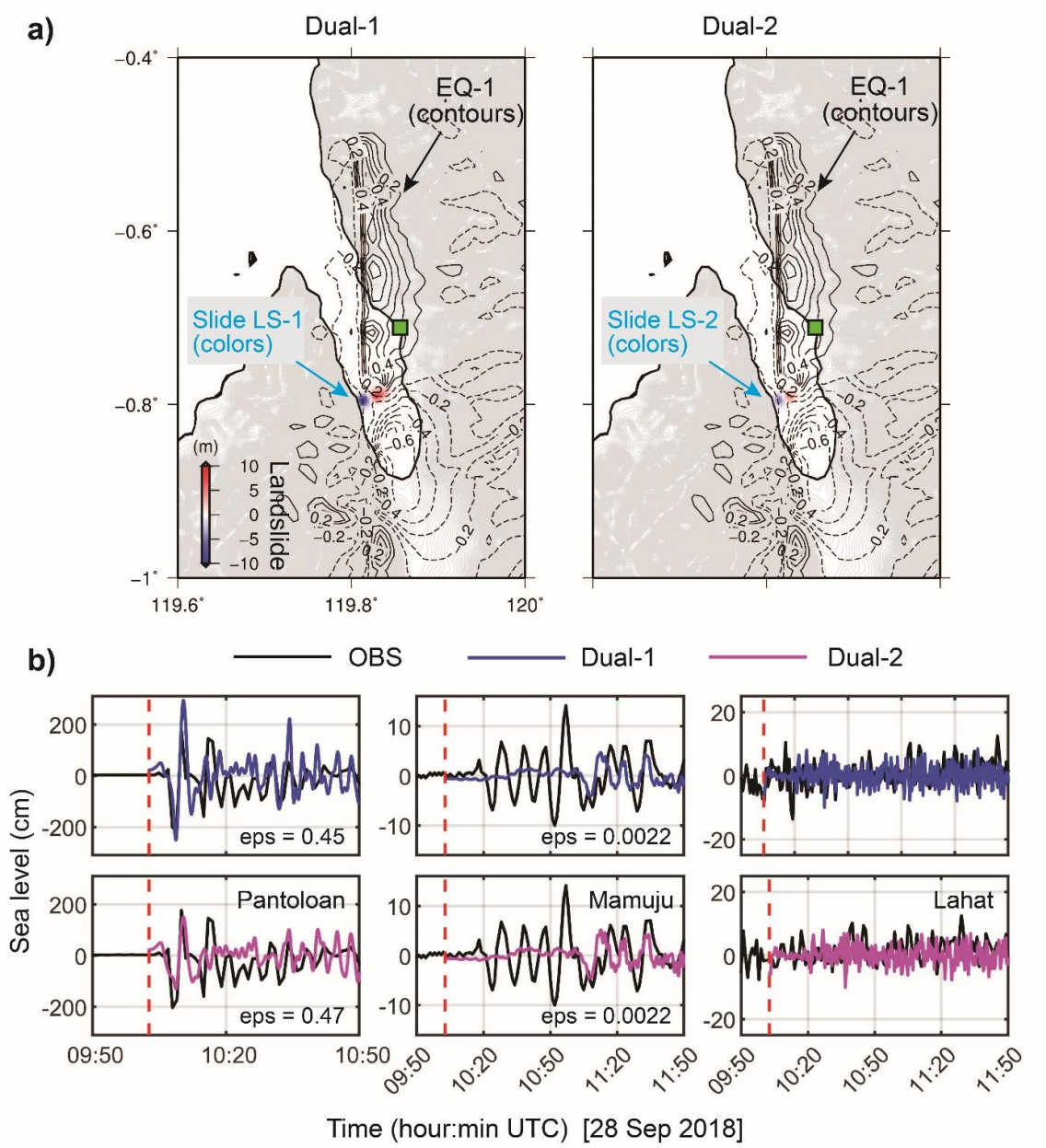

Figure 4. a) Two dual (combined earthquake and submarine landslide) source models Dual-1 and Dual-2, which are the combination of EQ-1 with LS-1 and LS-2, respectively, with corresponding crustal deformation and initial sea surface displacements. **b)** Comparison of observed and modelled tsunami waveforms at three tide gauge stations due to the two aforementioned dual source models. "eps" indicates misfit ϵ based on Equation (1). Misfits ("eps") are not calculated for Lahat as the tsunami signal is not clear at this station.

4. Modelling results and analysis

In this section, we compare modelling results with available observations of the 2018 Palu tsunami. Despite great importance of the 2018 Palu tsunami, the existing observation data of the tsunami is limited. In the near-field, two tide gauge observations are available at Pantoloan and Mamuju (Figure 1); however, the Mamuju record is outside of the Palu Bay and thus is most likely unaffected by the waves from the landslide source of the tsunami as the landslide waves are mostly confined within the Palu Bay (Heidarzadeh et al., 2019). In addition, the Mamuju record has a clock error of approximately 1 h. The Lahat Datu (abbreviated as "Lahat") tide gauge station, located approximately 600 km to the north of epicentre, does not show any tsunami signal (Figure 2b). The other observation available for the Palu tsunami is data of tsunami runup height surveys conducted by several authors following the tsunami (e.g., Arikawa et al. 2018; Muhari et al., 2018; Omira et al., 2019).

Before we discuss the results of simulations, it is helpful to note that, because the existing observation data of the Palu event is very limited, they can be reproduced by different types of source models. This is the reason that a large number of source models with different combinations have been proposed so far for this event (Table 1). Possibly the truth about the source mechanism of the 2018 Palu event may not emerge until high-resolution bathymetric and seismic surveys, accompanied with seafloor coring of the Palu Bay, are conducted.

297 **4.1 Performance of the earthquake source models (EQ-1, -2, and -3)**

298 Comparisons of the simulated waveforms and coastal heights from the three earthquake source
299 models are shown in Figures 2b and 5, respectively. Among the three earthquake models, Figure 2b
300 reveals that EQ-1 performs better compared to EQ-2 and -3 as the misfit resulting from EQ-1 at the
301 Pantoloan station (eps = 0.28) is significantly smaller than that from EQ-2 (eps = 2.67) and EQ-3 (eps
302 = 2.35). All the three earthquake models are unsuccessful in reproducing the Mamuju tide gauge
303 record in terms of wave amplitudes and arrival times. Heidarzadeh et al. (2019) speculated that either
304 the Mamuju tide gauge record has a clock error, or the early tsunami waves were due to a secondary
305 source such as a submarine landslide that occurred outside of the Palu Bay. Regarding the Lahat Datu
306 station, all models produce very small waves. It is important to note that the EQ-1 model reproduces
307 the initial phase and the period of the observation, but fails in matching the amplitude. All three
308 models significantly underestimate the surveyed runup (Figure 5). These are strong evidence that
309 indicate a secondary source (e.g., coseismic landslide) was most likely involved.

310

311 **4.2 Performance of the landslide source models (LS-1 and LS-2)**

312 Although it is clear that the 2018 Palu event was due to a dual source (combined earthquake and
313 landslide), here we present the simulation results of candidate landslide models with the aim of
314 understanding the nature of waves generated by submarine landslides. The simulation results for two
315 candidate landslide scenarios (LS-1 and LS-2) are shown in Figures 3b and 6. The model LS-2
316 significantly underestimates the Pantoloan tide gauge record (Figure 3b) and coastal heights (Figure

317 6). The misfit resulting from LS-1 at the Pantoloan station is 0.24 whereas it is 0.39 for LS-2 (Figure
318 3). However, the purpose of this section is not to rule out any of the LS-1 or LS-2 scenarios because
319 although they may not reproduce the observations, it is likely that a combination of them with an
320 earthquake model could reproduce the observations. This is discussed in the next section.
321
322 **4.3 Performance of the dual source models (Dual-1 and Dual-2)**
323 For our dual model, we combine the earthquake model EQ-1 with the two landslide models LS-1
324 and LS-2 and produce two dual models: Dual-1 and Dual-2 (Table 4). The basis for choosing EQ-1 for
325 making the dual models is that EQ-1 is the only earthquake model that successfully reproduces the
326 initial phases of the observed tsunami on the Pantoloan tide gauge (Figure 2b). Simulation results for
327 the dual models reveal that the model Dual-1 slightly overestimates the observed tide gauge waveform
328 (Figure 4b) and slightly underestimates the surveyed runup heights (Figure 6). However, its
329 performance is far better than that of the model Dual-2. In terms of waveform match at the Pantoloan
330 station, model Dual-1 gives a misfit of 0.45 whereas Dual-2 results in a misfit of 0.47 (Figure 4). For
331 runup, the misfits are 5.75 for Dual-1 and 7.68 for Dual-2 (Figure 6). It is noted that our model Dual-1
332 underestimates some runup measurement points including a few locations at the southwest of the Palu
333 Bay. By considering uncertainties associated with field measurements of runup heights and numerical
334 simulations, we may conclude that model Dual-1 can approximately reproduce the observations.
335

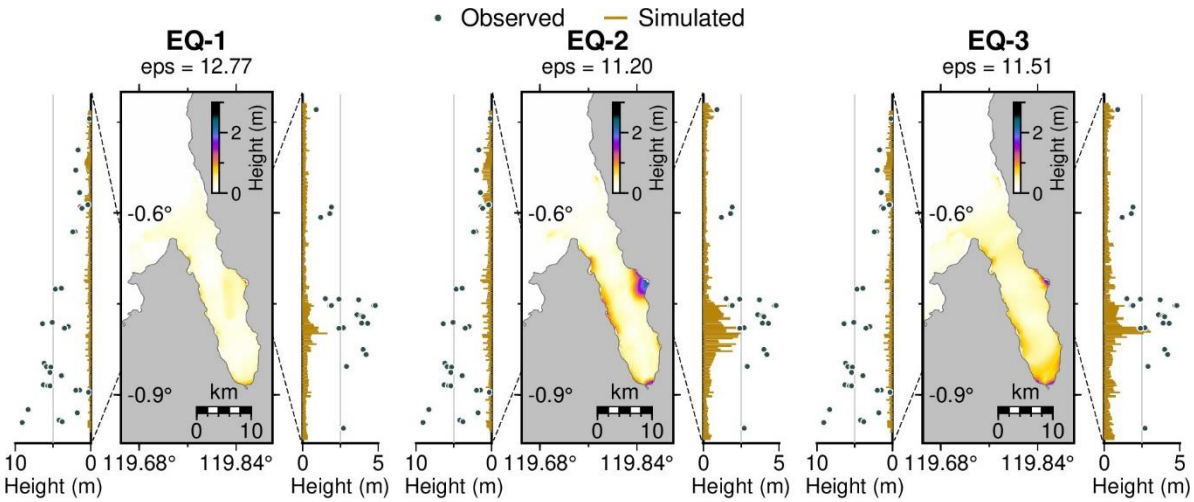

Figure 5. Comparison of simulated and observed runup for three earthquake-only source models EQ-1, EQ-2, and EQ-3. The observed data (i.e., circles) is based on Omira et al. (2019). "eps" indicates misfit ϵ based on Equation (1).

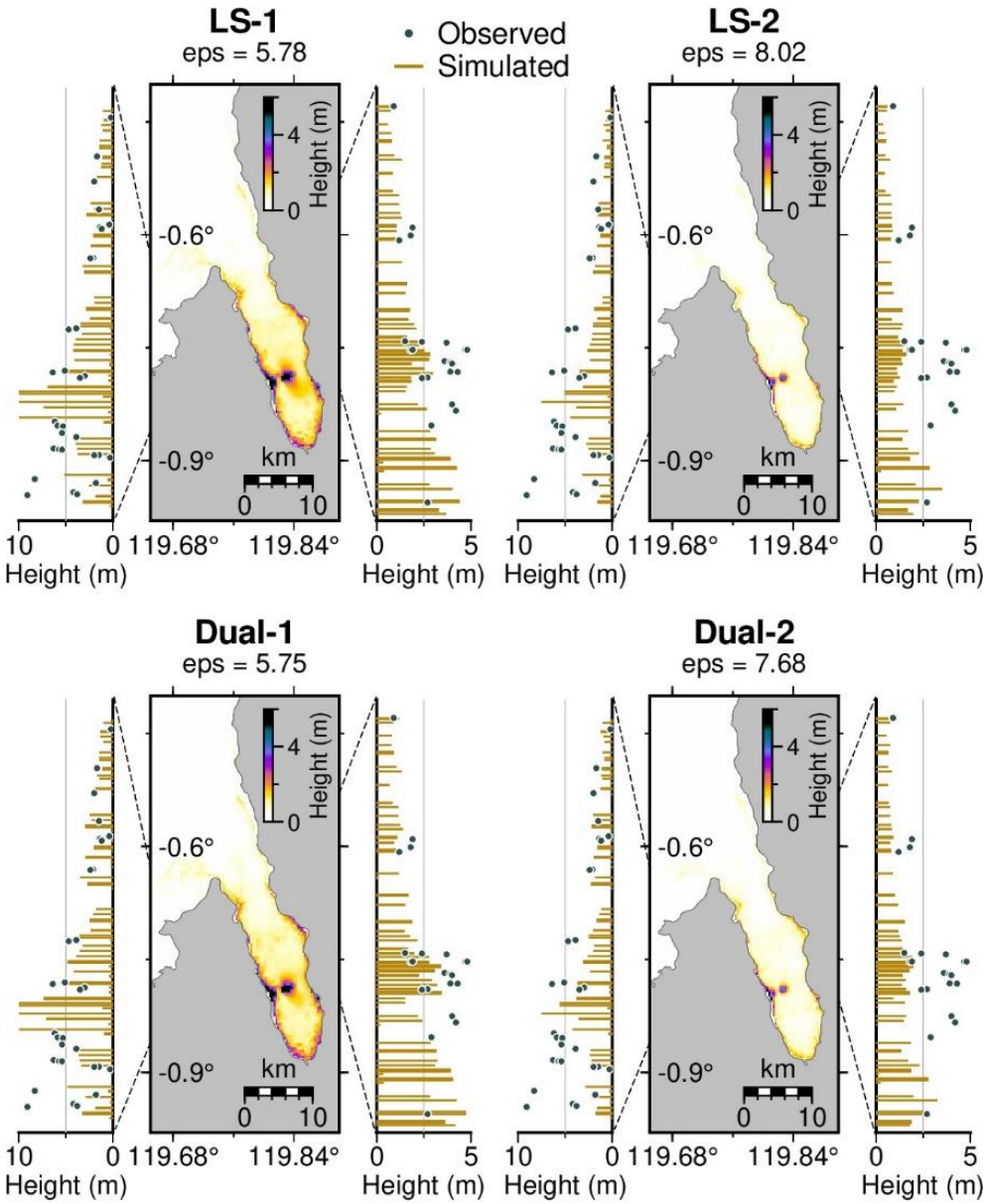

Figure 6. Top) Comparison of simulated and observed runup for two landslide-only source models LS-1 and LS-2. **Bottom)** Comparison of simulated and observed runup for two dual (combined earthquake and landslide) source models Dual-1 and Dual-2. The observed data (i.e., circles) is based on Omira et al. (2019). "eps" indicates misfit ϵ based on Equation (1).

5. Discussions

In addition to our final dual model, Dual-1 in Table 4 and Figure 4, three more dual models were proposed in the past few years by Heidarzadeh et al. (2019), Schambach et al. (2021), and Williamson et al. (2020) (Table 1). There are two differences between our model (Dual-1) and the other three modes: (1) our model is based on a credible submarine landslide (supported by an actual post-event bathymetric survey) while the other three models either only involve coastal subaerial landslides or include a hypothetical submarine landslide; (2) our model includes a single large submarine landslide whereas the other models incorporate seven (Schambach et al., 2021) and 11 (Williamson et al., 2020) coastal landslides although the model by Williamson et al. (2020) also involves a hypothetical submarine landslide whose location was previously proposed by Heidarzadeh et al. (2019).

Similar to this study, the dual models of Schambach et al. (2021) and Williamson et al. (2020) are also validated using tide gauge records and runup data. By comparing the results of modelling from our dual model, Dual-1 in Table 4 and Figure 4, with those of the aforesaid models, it is found that all dual models approximately equally reproduce the observation data, and it is hard to differentiate them in terms of quality of fit between simulations and observations. This may appear unexpected given the significant difference among these dual models. We speculate that such little differences among the results of different dual models could be attributed to: (i) Tsunami observations for the 2018 Palu event are sparse and scant; thus, do not provide sufficient redundancy to distinguish among models; and (ii) The Palu Bay area is a very narrow and small basin (length and width of the Palu Bay are

371 approximately 30 km and 7 km, respectively); therefore, different external forcings in a similar range
372 (such as the three dual models discussed here) may not be distinguishable by this small basin.
373 From a natural hazard mitigation point of view, it is important to note that the largest tsunami
374 heights and damage were due to the submarine landslide rather than the earthquake (Figures 5-6). For
375 example, Figure 5 shows that the earthquake-only models produce maximum runup heights of
376 approximately 2 m whereas the observed runup heights were more than 10 m. In fact, the 2018 Palu
377 catastrophe was mostly generated by the submarine landslide which was triggered by the earthquake.
378 This is called a cascading effect in the natural hazards literature where a primary hazard (earthquake)
379 cascades to other hazards (landslide) (Adams and Heidarzadeh, 2021; Heidarzadeh and Rabinovich,
380 2020) (Figure 7).
381

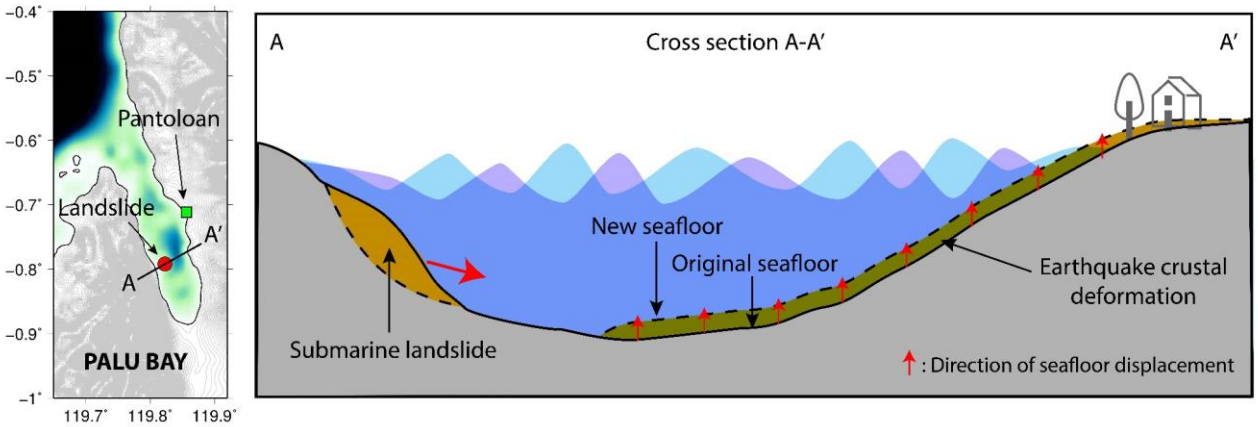

382
383 **Figure 7.** Sketch showing the final dual (earthquake and submarine landslide) model proposed in this
384 study for the 28 September 2018 Palu (Sulawesi) tsunami. This sketch highlights the cascading
385 multi-hazard nature of the 2018 Palu tsunami catastrophe.
386

6. Conclusions

We studied the source mechanism of the 2018 Palu (Sulawesi) tsunami through a numerical modelling approach accompanied with validation of the modelling results using observation data. Main findings are:

- Since limited observations are available for the 2018 Palu tsunami, they could be reproduced by multiple source models of different types (earthquake, landslide, and dual models). This is likely the reason that several source models are published for this tsunami.
- The earthquake source of the tsunami underestimates the surveyed runup by an order of magnitude, which indicates that a secondary source (e.g., a landslide) was most likely involved. Therefore, we conclude that the tsunami was most likely the result of a dual earthquake and landslide source.
- Although most of the existing landslide models for the Palu event are of the type of subaerial coastal landslides, we show that the existing tsunami observations can be approximately reproduced using a submarine landslide located inside the Palu Bay whose location is confirmed through marine bathymetric surveys.
- Our final dual model comprises of the USGS earthquake model and a submarine landslide. The USGS earthquake model has a length of 264 km, width of 37 km and a slip in the range of 0 – 8.5 m. The submarine landslide model has a length of 1.0 km width of 2.0 km and a thickness of 80.0 m located at 119.823 ^{o}E and -0.792 ^{o}S.

Acknowledgements

A number of figures were drafted using the GMT software (Wessel and Smith, 1998).

Funding

This research is funded by the Royal Society (the United Kingdom) grant number CHL/R1/180173. Additional funding received from the Lloyd's Tercentenary Research Foundation, the Lighthill Risk Network, and the Lloyd's Register Foundation-Data Centric Engineering Programme of the Alan Turing Institute (UK).

Data and Resources

All data used in this study are given in the body of the article.

Declaration of interest

The authors declare that they have no competing interests regarding the work presented in this paper.

References

Adams, K., M. Heidarzadeh. 2021. "A multi-hazard risk model with cascading failure pathways for the Dawlish (UK) railway using historical and contemporary data". International Journal of Disaster

425 Risk Reduction 56: 102082. https://doi.org/10.1016/j.ijdrr.2021.102082.

426 Aránguiz, R., M. Esteban, H. Takagi, T. Mikami, T. Takabatake, M. Gómez, J. González, T.
427 Shibayama, R. Okuwaki, Y. Yagi, K. Shimizu. 2020. "The 2018 Sulawesi tsunami in Palu city as
428 a result of several landslides and coseismic tsunamis." Coastal Engineering Journal 62(4): 445-
429 459.

430 Arikawa, T., A. Muhari, Y. Okumura, Y. Dohi, B. Afriyanto, K. A. Sujatmiko, F. Imamura. 2018.
431 "Coastal subsidence induced several tsunamis during the 2018 Sulawesi earthquake." Journal of
432 Disaster Research 13: sc20181201.

433 Courant, R., K. Friedrichs, H. Lewy. 1928. "Über die partiellen Differenzengleichungen der
434 mathematischen Physik." Mathematische Annalen 100 (1): 32-74.

435 Frederik, M.C.G., Udrekh, R. Adhitama, N. D. Hananto, Asrafil, S. Sahabuddin, M. Irfan, O. Moefti,
436 D. B. Putra, and B. F. Riyalda. 2019. "First Results of a Bathymetric Survey of Palu Bay, Central
437 Sulawesi, Indonesia following the Tsunamigenic Earthquake of 28 September 2018." Pure and
438 Applied Geophysics 176: 3277–3290. https://doi.org/10.1007/s00024-019-02280-7.

439 Fujii, Y., K. Satake. 2006. "Source of the July 2006 West Java tsunami estimated from tide gauge
440 records." Geophysical Research Letters 33 (24).

441 Geoware. 2011. "The tsunami travel times (TTT) package." Available at http://www.geoware-
442 online.com/tsunami.html.

443 Grilli, S. T., C. Zhang, J. T. Kirby, A. R. Grilli, D. R. Tappin, S. F. Watt, et al. 2021. "Modeling of the

444 Dec. 22nd 2018 Anak Krakatau volcano lateral collapse and tsunami based on recent field
445 surveys: Comparison with observed tsunami impact." Marine Geology 440:
446 doi:10.1016/j.margeo.2021.106566.
447 Gusman, A. R., P. Supendi, A. D. Nugraha, W. Power, H. Latief, H. Sunendar, et al. 2019. "Source
448 model for the tsunami inside Palu Bay following the 2018 Palu earthquake, Indonesia."
449 Geophysical Research Letters 46: 8721–8730. https://doi.org/10.1029/ 2019GL082717.
450 He, L., G. Feng, Z. Li, Z. Feng, H. Gao, X. Wu. 2019. "Source parameters and slip distribution of the
451 2018 Mw 7.5 Palu, Indonesia earthquake estimated from space-based geodesy." Tectonophysics
452 772: 228216.
453 Heidarzadeh, M., A.R. Gusman, A. Patria, B. T. Widyantoro. 2022. "Potential landslide origin of the
454 Seram Island tsunami in Eastern Indonesia on 16 June 2021 following an Mw 5.9 earthquake".
455 Bulletin of the Seismological Society of America, https://doi.org/10.1785/0120210274.
456 Heidarzadeh, M., K. Satake. 2015. "Source properties of the 17 July 1998 Papua New Guinea tsunami
457 based on tide gauge records." Geophysical Journal International 202 (1): 361-369.
458 Heidarzadeh, M., K. Satake. 2017. "A Combined Earthquake-Landslide Source Model for the Tsunami
459 from the 27 November 1945 M 8.1 Makran Earthquake." Bulletin of the Seismological Society of
460 America 107 (2): 1033-1040. https://doi.org/10.1785/0120160196.
461 Heidarzadeh, M., A. Muhari, A. B. Wijanarto. 2019. "Insights on the source of the 28 September 2018
462 Sulawesi tsunami, Indonesia based on spectral analyses and numerical simulations." Pure and

463 Applied Geophysics 176: 25–43. https://doi.org/10.1007/s00024-018-2065-9.

464 Heidarzadeh, M., A. B. Rabinovich. 2020. “Combined Hazard of Typhoon-Generated Meteorological
465 Tsunamis and Storm Surges along the Coast of Japan”. Natural Hazards 106: 1639–
466 1672. https://doi.org/10.1007/s11069-020-04448-0.

467 Heidarzadeh, M., T. Ishibe, O. Sandanbata, A. Muhari, and A. B. Wijanarto. 2020. “Numerical
468 modeling of the subaerial landslide source of the 22 December 2018 Anak Krakatoa volcanic
469 tsunami, Indonesia.” Ocean Engineering 195: 106733.
470 https://doi.org/10.1016/j.oceaneng.2019.106733.

471 Jamelot, A., A. Gailler, P. Heinrich, A. Vallage, J. Champenois. 2019. “Tsunami simulations of the
472 Sulawesi Mw 7.5 event: comparison of seismic sources issued from a tsunami warning context
473 versus post-event finite source.” Pure and Applied Geophysics 176(8): 3351-3376.

474 Lee, S. J., T. P. Wong, T. C. Lin, T. Y. Liu. 2019. “Complex triggering supershear rupture of the
475 2018 M W 7.5 Palu, Indonesia, earthquake determined from teleseismic source
476 inversion.” Seismological Research Letters 90(6): 2111-2120.

477 Liu, P. F., P. Higuera, S. Husrin, G. S. Prasetya, J. Prihantono, H. Diastomo, et al. 2020. “Coastal
478 landslides in Palu Bay during 2018 Sulawesi earthquake and tsunami.” Landslides 17(9): 2085-
479 2098.

480 Muhari, A., F. Imamura, T. Arikawa, A. R. Hakim, B. Afriyanto. 2018. “Solving the puzzle of the
481 September 2018 Palu, Indonesia, tsunami mystery: clues from the tsunami waveform and the

initial field survey data." Journal of Disaster Research 13: sc20181108.

Mulia, I. E., S. Watada, T. -C. Ho, K. Satake, Y. Wang, A. Aditiya. 2020. "Simulation of the 2018 tsunami due to the flank failure of Anak Krakatau volcano and implication for future observing systems." Geophysical Research Letters 47: e2020GL087334. https://doi.org/10.1029/2020GL087334.

Nakata, K., A. Katsumata, A. Muhari. 2020. "Submarine landslide source models consistent with multiple tsunami records of the 2018 Palu tsunami, Sulawesi, Indonesia." Earth Planets and Space 72(1): 1-16.

Natawidjaja, D. H., M. R. Daryono, G. Prasetya, P. L. Liu, N. D. Hananto, W. Kongko, et al. 2021. "The 2018 M w7. 5 Palu 'supershear'earthquake ruptures geological fault's multisegment separated by large bends: results from integrating field measurements, LiDAR, swath bathymetry and seismic-reflection data." Geophysical Journal International 224 (2): 985-1002.

Okada Y. 1985. "Surface deformation due to shear and tensile faults in a half-space." Bulletin of the Seismological Society of America 75: 1135–1154.

Okal, E. A., C. E. Synolakis. 2004. "Source discriminants for near-field tsunamis." Geophysical Journal International 158(3): 899–912. https://doi.org/10.1111/j.1365-246X.2004.0247.x .

Omira, R., G. G. Dogan, R. Hidayat, S. Husrin, A. Annunziato, C. Proietti, P. Probst, M. A. Paparo, M. Wronna, A. Zaytsev, A. C. Yalciner, et al. 2019. "The September 28th, 2018, tsunami in Palu-Sulawesi, Indonesia: A post-event field survey." Pure and Applied Geophysics 176(4): 1379-

1395.

Pakoksung, K., A. Suppasri, F. Imamura, C. Athanasius, A. Omang, A. Muhari. 2019. “Simulation of the submarine landslide tsunami on 28 September 2018 in Palu Bay, Sulawesi Island, Indonesia, using a two-layer model.” Pure and Applied Geophysics 176(8): 3323-3350.

Pranantyo, I.R., M. Heidarzadeh, P.R. Cummins. 2021. “Complex tsunami hazards in eastern Indonesia from seismic and non-seismic sources: Deterministic modelling based on historical and modern data”. Geoscience Letters, 8(1): 1-16. https://doi.org/10.1186/s40562-021-00190-y

Satake, K., M. Heidarzadeh, M. Quiroz, R. Cienfuegos. 2020. “History and features of trans-oceanic tsunamis and implications for paleo-tsunami studies.”” Earth-Science Reviews: https://doi.org/10.1016/j.earscirev.2020.103112.

Satake, K., Y. Tanioka. 2003. “The July 1998 Papua New Guinea earthquake: Mechanism and quantification of unusual tsunami generation.” Pure and Applied Geophysics 160 (10): 2087-2118.

Satake, K., Y. Nishimura, P. S. Putra, A. R. Gusman, H. Sunendar, Y. Fujii, Y., et al. 2013. “Tsunami source of the 2010 Mentawai, Indonesia earthquake inferred from tsunami field survey and waveform modeling.” Pure and Applied Geophysics 170 (9–10): 1567–1582.

Schambach, L., S. T. Grilli, D. R. Tappin. 2021. “New high-resolution modeling of the 2018 Palu tsunami, based on supershear earthquake mechanisms and mapped coastal landslides, supports a dual source.” Frontiers in Earth Science 8: 627.

520 Somphong, C., A. Suppasri, K. Pakoksung, T. Nagasawa, Y. Narita, R. Tawatari, et al. 2022.
521 "Submarine landslide source modeling using the 3D slope stability analysis method for the 2018
522 Palu, Sulawesi, tsunami." Natural Hazards and Earth System Sciences 22(3): 891-907.
523 Syamsidik, Benazir, M. Umar, G. Margaglio, A. Fitrayansyah. 2019. "Post-tsunami survey of the 28
524 September 2018 tsunami near Palu Bay in Central Sulawesi, Indonesia: Impacts and challenges to
525 coastal communities." International Journal of Disaster Risk Reduction 38: 101229.
526 Synolakis, C. E., J. P. Bardet, J. C. Borrero, H. L. Davies, E. A. Okal, E. A. Silver, E. A. Silver, S.
527 Sweet, and D. R. Tappin. 2002. "The slump origin of the 1998 Papua New Guinea
528 tsunami." Proceedings of Royal Society of London A 458: 763-789.
529 Takagi, H., M. B. Pratama, S. Kurobe, M. Esteban, R. Aránguiz, B. Ke. 2019. "Analysis of generation
530 and arrival time of landslide tsunami to Palu City due to the 2018 Sulawesi
531 earthquake." Landslides 16(5): 983-991.
532 Tappin, D. R., P. Watts, S. T. Grilli. 2008. "The Papua New Guinea tsunami of 17 July 1998: anatomy
533 of a catastrophic event." Natural Hazards and Earth System Sciences 8 (2): 243-266.
534 Tinti, S., A. Armigliato, A. Manucci, G. Pagnoni, F. Zaniboni, A.C. Yalçiner, Y. Altinok. 2006. "The
535 generating mechanisms of the August 17, 1999 izmit bay (turkey) tsunami: Regional (tectonic)
536 and local (mass instabilities) causes". Marine Geology 225(1–4): 311–330.
537 https://doi.org/10.1016/j.margeo.2005. 09.010.
538 Ulrich, T., S. Vater, E. H. Madden, J. Behrens, Y. van Dinther, I. Van Zelst, E. J. Fielding, C. Liang, A-

539 A. Gabriel. 2019. “Coupled, physics-based modeling reveals earthquake displacements are
540 critical to the 2018 Palu, Sulawesi tsunami.” Pure and Applied Geophysics 176 (10): 4069-4109.
541 USGS (The United States Geological Survey). 2018. “Finite Fault Model for M 7.5 - 72 km N of Palu,
542 Indonesia.” Available online at:
543 https://earthquake.usgs.gov/earthquakes/eventpage/us1000h3p4/finite-fault (accessed on 21
544 December 2021).
545 Wang, X., P. L.-F. Liu. 2006. “An analysis of 2004 Sumatra earthquake fault plane mechanisms and
546 Indian Ocean tsunami.” Journal of Hydraulic Research 44: 147–154.
547 Wang, Y., W. Feng, K. Chen, S. Samsonov. 2019. “Source characteristics of the 28 September 2018
548 Mw 7.4 Palu, Indonesia, earthquake derived from the advanced land observation satellite 2
549 data.” Remote Sensing 11(17): 1999.
550 Watts, P., S. T. Grilli, D. R. Tappin, G. J. Fryer. 2005. “Tsunami generation by submarine mass failure.
551 II: Predictive equations and case studies.” Journal of Waterway Port Coastal and Ocean
552 Engineering 131 (6): 298-310.
553 Weatherall P., K. M. Marks, M. Jakobsson, et al. 2015. “A new digital bathymetric model of the
554 world’s oceans.” Earth Space Science 2: 331–345.
555 Wessel, P., W. H. F. Smith. 1998. “New, improved version of generic mapping tools released.” EOS
556 Transactions of AGU 79 (47): 579.
557 Williamson, A. L., D. Melgar, X. Xu, C. Milliner. 2020. “The 2018 Palu tsunami: Coeval landslide and

558 coseismic sources." Seismological Society of America 91(6): 3148-3160.

559 Yolsal-Çevikbilen, S., T. Taymaz. 2019. "Source characteristics of the 28 September 2018 Mw 7.5

560 Palu-Sulawesi, Indonesia (SE Asia) earthquake based on inversion of teleseismic body

561 waves." Pure and Applied Geophysics 176 (10): 4111-4126.

562

Table captions

Table 1. A list of some of the published source models for the September 2018 Palu (Sulawesi) tsunami.

Table 2. Earthquake source models used in this study for modelling the 28 September 2018 Palu (Sulawesi) earthquake and tsunami.

Table 3. Parameters of the two landslide scenarios considered in this study for modelling the 28 September 2018 Palu (Sulawesi) tsunami.

Table 4. Information of two dual earthquake and landslide source models considered in this study for modelling the 28 September 2018 Palu (Sulawesi) tsunami.

*** End of Table captions ***

Figure captions

Figure 1. Map showing Eastern Indonesia, the site of the 28 September 2018 Palu (Sulawesi) earthquake and tsunami. The red star indicates the epicenter of the earthquake, the green squares are the locations of tide gauge stations, and the dashed contours show the tsunami travel times (TTT) in minutes calculated using the TTT software of Geoware (2011). The Palu-Koro strike-slip fault system (PKF) is shown by a dashed thick straight line. The focal mechanism is based on the United States Geological Survey (USGS) catalogue. The pink rectangle demonstrates the fault extension for the 2018 Palu earthquake based on Lee et al. (2019).

Figure 2. a) Three published seismic source models for the 28 September 2018 Palu (Sulawesi) M_w 7.5 earthquake namely EQ-1 (USGS, 2018), EQ-2 (Jamelot et al., 2019), and EQ-3 (Wang et al., 2019). **b)** Comparison of observed and modelled tsunami waveforms at three tide gauge stations due to the three aforementioned earthquake source models. “U” and “S” denote “uplift” and “subsidence”, respectively. “eps” indicates misfit ϵ based on Equation (1). Misfits (“eps”) are not calculated for Lahat as the tsunami signal is not clear at this station.

Figure 3. a) Two landslide models LS-1 and LS-2 considered in this study with corresponding initial sea surface displacements. **b)** Comparison of observed and modelled tsunami waveforms at three tide gauge stations due to the two aforementioned landslide scenarios. “eps” indicates misfit ϵ based on Equation (1). Misfits (“eps”) are not calculated for Mamuju and Lahat as the simulated waves are very small at these stations.

Figure 4. a) Two dual (combined earthquake and submarine landslide) source models Dual-1 and Dual-2, which are the combination of EQ-1 with LS-1 and LS-2, respectively, with corresponding crustal deformation and initial sea surface displacements. **b)** Comparison of observed and modelled tsunami waveforms at three tide gauge stations due to the two aforementioned dual source models. "eps" indicates misfit ϵ based on Equation (1). Misfits ("eps") are not calculated for Lahat as the tsunami signal is not clear at this station.

Figure 5. Comparison of simulated and observed runup for three earthquake-only source models EQ-1, EQ-2, and EQ-3. The observed data (i.e., circles) is based on Omira et al. (2019). "eps" indicates misfit ϵ based on Equation (1).

Figure 6. Top) Comparison of simulated and observed runup for two landslide-only source models LS-1 and LS-2. **Bottom)** Comparison of simulated and observed runup for two dual (combined earthquake and landslide) source models Dual-1 and Dual-2. The observed data (i.e., circles) is based on Omira et al. (2019). "eps" indicates misfit ϵ based on Equation (1).

Figure 7. Sketch showing the final dual (earthquake and submarine landslide) model proposed in this study for the 28 September 2018 Palu (Sulawesi) tsunami. This sketch highlights the cascading multi-hazard nature of the 2018 Palu tsunami catastrophe.

*** End of Figure captions ***